

# Photoluminescence properties of midinfrared dilute nitride InAsN epilayers with/without Sb flux during molecular beam epitaxial growth

Rui Chen,<sup>1</sup> S. Phann,<sup>1</sup> H. D. Sun,<sup>1,a)</sup> Q. Zhuang,<sup>2</sup> A. M. R. Godenir,<sup>2</sup> and A. Krier<sup>2</sup>

<sup>1</sup>Division of Physics and Applied Physics, School of Physical and Mathematical Sciences, Nanyang Technological University, Singapore 637371, Singapore

<sup>2</sup>Department of Physics, Lancaster University, Lancaster LA1 4YB, United Kingdom

(Received 23 October 2009; accepted 9 December 2009; published online 30 December 2009)

We report on the comparative studies of photoluminescence (PL) properties of molecular beam epitaxy grown dilute InAsN epilayers with and without antimony (Sb) flux during the growth. Both samples exhibit strong midinfrared (MIR) emission at room temperature, while the sample with Sb flux has much higher intensity. At low temperatures, these samples exhibit totally different PL features in terms of line width, peak position, intensity, and their dependences on temperature and excitation density. Our results clearly indicate that part of Sb atoms serve as a surfactant that effectively improves the optical quality of MIR dilute nitrides. © 2009 American Institute of Physics. [doi:10.1063/1.3280861]

The addition of a small fraction of nitrogen into III-V compounds to form the so-called dilute nitride semiconductors has attracted substantial research attention since the 1990s due to their unusual fundamental physical properties and potential applications in optoelectronics and photonics.<sup>1,2</sup> Narrow band gap InAsN material is technologically important for applications in the midinfrared region from 2 to 5  $\mu\text{m}$ , such as free space communication, environmental monitoring, molecular spectroscopy, etc.<sup>3</sup> Due to the difficulty in the fabrication of high quality materials, it is only recently that the room temperature emission from InAsN thin films has been realized.<sup>4–10</sup> However, the growth of InAsN is still challenging, and the difficulties in suppressing nonradiative recombination centers or phase separation must be overcome in order to further improve the material quality. Different approaches including optimizing epitaxial parameters<sup>6</sup> and postgrowth thermal annealing<sup>11</sup> have been adopted to present such efforts. More recently, the employment of antimony (Sb) during the growth of InAsN has been reported, and 4.0  $\mu\text{m}$  InAsN:Sb/InAs *p-i-n* light emitting diodes at low temperature have been demonstrated.<sup>12</sup> Nevertheless, there has been no detailed investigation into the role of Sb on the optical properties in this material. In this letter, the effect of Sb during the epitaxial growth is elucidated by comparative studies of temperature- and excitation intensity-dependent photoluminescence (PL) spectra of samples with and without Sb flux during growth. It is clarified that Sb atoms can both go into the crystal lattice to tune the band gap and act as a surfactant, which greatly improves the optical quality of the epilayer.

The samples of 1- $\mu\text{m}$ -thick InAsN(Sb) epilayers were fabricated on InAs substrates by solid source molecular beam epitaxy using a radio frequency plasma nitrogen source. The growth temperature was set to be 420 °C and growth rate of 1.0  $\mu\text{m}/\text{h}$ , under a fixed As flux of  $2.2 \times 10^{-6}$  mbar with a fixed nitrogen plasma setting, a power of 160 W, and nitrogen flux of  $5.0 \times 10^{-7}$  mbar. A valved cracker cell was used to vary Sb flux. The N concentration in the epilayers was

deduced from the high resolution double crystal x-ray diffraction. Detailed investigation of the N concentration of the samples and other relevant information of the sample growth can be found in Refs. 6 and 12. The temperature dependent PL measurements were performed through a closed cycle helium cryostat with sapphire windows. A diode laser emitting at 660 nm was used as the PL excitation source and the PL signal was dispersed by a 300 mm monochromator combined with suitable filters and detected by a liquid-nitrogen-cooled InSb photodiode detector using the standard lock-in amplifier technique.

In this study, we focus on two samples. One is InAsN without Sb flux during growth with nitrogen concentration of 1.4% (sample A) and the other one is InAsN:Sb having the same nitrogen concentration but with Sb flux during growth (sample B). The nominal Sb concentration in sample B is 4.1%, as determined by energy dispersive x-ray spectrometry and electron probe microanalysis. Figure 1 shows the room temperature PL spectra of the samples under a laser excitation density around  $35 \text{ W cm}^{-2}$ , and the inset is the PL obtained at 10 K. The double peaks feature of the emission near 4.25  $\mu\text{m}$  is due to atmospheric  $\text{CO}_2$  absorption in the optical path. The spectra of the sample without Sb (sample A) present low intensity and broad line width, which is common

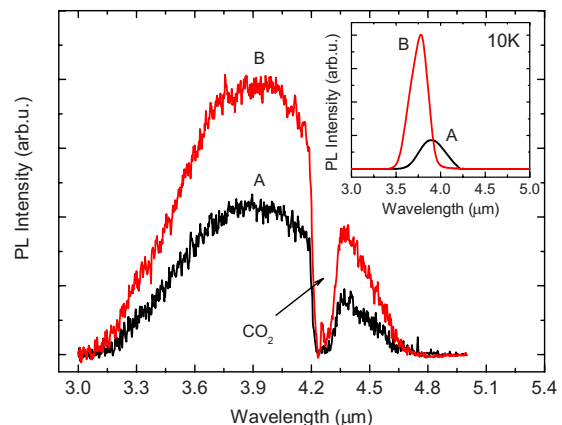


FIG. 1. (Color online) PL spectra of sample A and B measured at room temperature and at 10 K (inset).

<sup>a)</sup>Author to whom correspondence should be addressed. Electronic mail: hdsun@ntu.edu.sg.

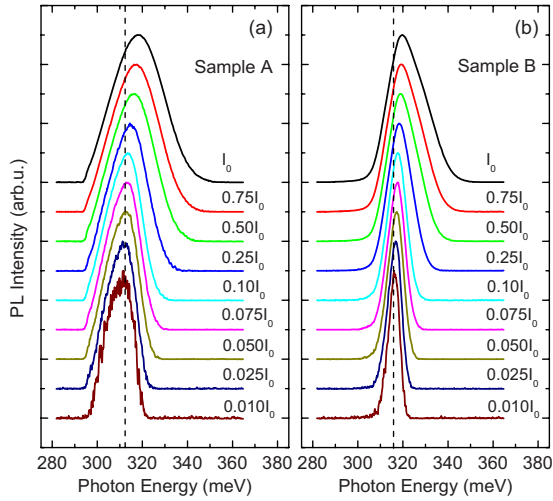


FIG. 2. (Color online) Evolution of the PL spectra measured at 10 K under different excitation densities. The dashed vertical lines are a guide for the eyes.

in dilute nitride materials.<sup>13</sup> Comparatively, the intensity of sample with Sb (sample B) is enhanced by about 1.7 times. Furthermore, at 10 K, sample B exhibits much smaller full width at half maximum (FWHM). The optical quality of sample B is apparently better than sample A as far as the PL intensity and line width is concerned.

Figure 2 depicts the PL spectra measured at 10 K under various excitation densities for sample A and B, respectively. It is noted that the FWHM of the PL of sample B is always smaller than sample A under the same conditions. For an excitation density increase by two orders of magnitude, sample A displays a gradual PL shift toward higher energy with a total shift about 6 meV. In comparison, sample B demonstrates a similar trend to sample A but the total shift is only 4 meV. In dilute nitride material, the band edge emission always presents an exponential tail in the joint density of states (DOS) due to the random potential fluctuations caused by N incorporation. At low temperature or low excitation densities, the photogenerated electrons are localized in these states. An increased excitation density then leads to the saturation of this band tail state and hence a blueshift of the emission band.<sup>14</sup> The amount of the shifts should be related to the distribution of the DOS; a larger one is related to deeper localization because they are far away from the conduction band edge.<sup>15</sup> It can be derived from the differences between the optical characterizations that sample B demonstrates shallower localization because the adoption of Sb could decrease the disorders in the crystalline structure and composition homogeneity and thus improve the material quality.<sup>16</sup>

In order to further investigate the effect of Sb on the optical properties of InAsN epilayer, temperature dependent PL measurement was carried out under a laser excitation density around  $35 \text{ W cm}^{-2}$ . The normalized PL spectra of samples measured in the temperature range between 10 and 240 K are shown in Figs. 3(a) and 3(b), respectively. Higher temperature data is not included for discussion because of the difficulty in peak assignment influenced by  $\text{CO}_2$  absorption. Peak positions of individual spectra are indicated by dashed lines. The peaks of both samples broaden and exhibit a blueshift followed by a redshift. It is noted that the PL spectra exhibit a pronounced broadening at high temperature,

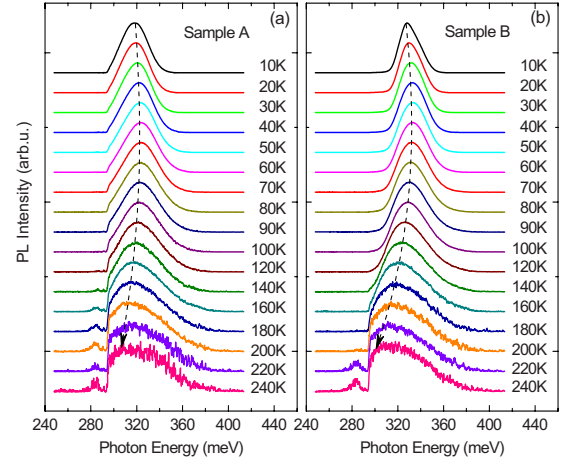


FIG. 3. (Color online) Temperature-dependent PL spectra for sample A (a) and B (b) measured at an excitation density of  $35 \text{ W cm}^{-2}$ . The dashed lines follow the peak positions.

which is due to the thermal distribution of carriers around the Fermi energy.<sup>9</sup>

Next, we look into detailed PL characteristics including emission peak energy and the integrated PL intensity as a function of temperature. Figure 4(a) shows corresponding peak energies of the samples. The dashed line is the InAs band gap shrinkage obtained from the empirical Varshni equation<sup>17</sup>

$$E_g(T) = E_g(0) - \alpha T^2 / (T + \beta) \quad (1)$$

with parameters of  $E_g(0)=415 \text{ meV}$ ,  $\alpha=0.276 \text{ meV/K}$  and  $\beta=83 \text{ K}$ ,<sup>18</sup> offsetted in the y axis for better comparison. A non-Varshni-like evolution of the PL peak position is observed for both samples, revealing the existence of localized states in the material system.<sup>19–21</sup> It can be seen clearly from Fig. 4(a) that the PL peaks of sample B initially shift toward higher energy before slowing down and then follow the conventional trend of InAs. This behavior is associated with

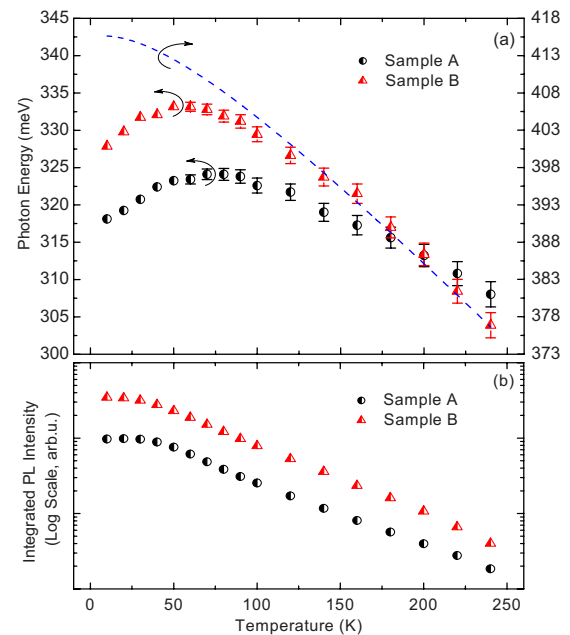


FIG. 4. (Color online) (a) Temperature dependents of the peak energies and (b) the integrated PL intensity of sample A and B, respectively. The dashed line in (a) is the InAs band gap shrinkage obtained from Varshni law.

localization of excitons at low temperatures. When the temperature increases, excitons with sufficient thermal energy can readily be detrapped from the localized states and reveal more characteristics of band to band recombination. Comparatively, sample A demonstrates much slower band gap shrinkage with temperature and apparently cannot be described by the Varshni equation even at high temperature. This suggests that the PL from sample A is not dominated by band gap emission but by the emission from localized carriers up to 200 K. The localization ability in sample A is quite strong (localization energy estimated to be  $\sim 17$  meV) and the carriers do not have enough thermal energy to detrapp at temperature lower than 200 K. This verifies that sample A has a deeper localization compared with sample B, which is consistent with the power dependent PL measurement depicted in Fig. 2.

Owing to the high nominal Sb concentration in sample B, we believe that a small amount of Sb atoms have been incorporated into the film during material growth. This is inferred from the crossing of the peak photon energy curves of sample A and B described in Fig. 4(a). It is well known that the replacement of As with N and Sb in III-V materials results in reduction of the band gap with the former lowering the conduction band and the latter lifting the valence band.<sup>22</sup> The crossing of the curves indicates that some of Sb atoms go into the crystal lattice to form quaternary alloy, because otherwise the high temperature (240 K) PL of sample B should be the same compared to sample A. All the data discussed above suggests that sample A demonstrates very deep carrier localization while the material quality has greatly improved by the introduction of Sb. There are two roles of Sb played during the material growth, one is that part of the Sb atoms float at the surface and serves as a surfactant, and the other one is that a small amount of Sb is incorporated into the lattice to tune the band gap of the material. Actually if all the Sb atoms are incorporated into the InAsN lattice, the band gap should have been reduced by about 30 meV.<sup>23</sup> It is obvious from Fig. 4(a) that the band gap reduction by Sb is only 4.5 meV, which verifies that only a small amount of Sb atoms ( $\sim 0.06\%$ ) go into the lattice to form quaternary alloy.

Finally, temperature dependence of the integrated PL intensity of the two samples is shown in Fig. 4(b). The approach of interpolation was used to exclude the influence of CO<sub>2</sub> absorption on the PL emission. It is shown that the integrated PL intensity of sample B is improved at all temperatures. Once again, the data provide evidences that Sb acts mainly in a surfactantlike manner lowering surface free energy, suppressing diffusion and preventing three-dimensional growth, island formation, and phase separation, and finally resulting in a better material quality.<sup>24,25</sup>

In summary, we have presented the optical property comparison of InAsN samples with and without Sb flux during epitaxial growth while containing the same nitrogen mole fraction. It has been observed that the PL intensity of the sample is remarkably improved and the localized state due to nitrogen incorporation has been greatly suppressed by the introduction of Sb. This improvement can be pushed further by an accurate optimization of growth parameters for device application.

- <sup>1</sup>S. Sakai, Y. Ueta, and Y. Terauchi, *Jpn. J. Appl. Phys., Part 1* **32**, 4413 (1993).
- <sup>2</sup>I. Vurgaftman and J. R. Meyer, *J. Appl. Phys.* **94**, 3675 (2003).
- <sup>3</sup>J. Wagner, C. Mann, M. Rattunde, and G. Weimann, *Appl. Phys. A: Mater. Sci. Process.* **78**, 505 (2004).
- <sup>4</sup>S. Dhar, T. D. Das, M. de la Mare, and A. Krier, *Appl. Phys. Lett.* **93**, 071905 (2008).
- <sup>5</sup>T. D. Veal, L. F. J. Piper, P. H. Jefferson, I. Mahboob, C. F. McConville, M. Merrick, T. J. C. Hosea, B. N. Murdin, and M. Hopkinson, *Appl. Phys. Lett.* **87**, 182114 (2005).
- <sup>6</sup>Q. Zhuang, A. M. R. Godenir, A. Krier, K. T. Lai, and S. K. Haywood, *J. Appl. Phys.* **103**, 063520 (2008).
- <sup>7</sup>M. Kuroda, A. Nishikawa, R. Katayama, and K. Onabe, *J. Cryst. Growth* **278**, 254 (2005).
- <sup>8</sup>Q. Zhuang, A. Godenir, and A. Krier, *J. Phys. D: Appl. Phys.* **41**, 132002 (2008).
- <sup>9</sup>M. de la Mare, Q. Zhuang, A. Krier, A. Patane, and S. Dhar, *Appl. Phys. Lett.* **95**, 031110 (2009).
- <sup>10</sup>D. K. Shih, H. H. Lin, L. W. Sung, T. Y. Chu, and T. R. Yang, *Jpn. J. Appl. Phys., Part 1* **42**, 375 (2003).
- <sup>11</sup>S. Shirakata, M. Kondow, and T. Kitatani, *Appl. Phys. Lett.* **80**, 2087 (2002).
- <sup>12</sup>Q. Zhuang, A. Godenir, A. Krier, G. Tsai, and H. H. Lin, *Appl. Phys. Lett.* **93**, 121903 (2008).
- <sup>13</sup>T. Kageyama, T. Miyamoto, S. Makino, F. Koyama, and K. Iga, *Jpn. J. Appl. Phys., Part 2* **38**, L298 (1999).
- <sup>14</sup>E. Kuokstis, J. Zhang, M. Y. Ryu, J. W. Yang, G. Simin, M. A. Khan, R. Gaska, and M. S. Shur, *Appl. Phys. Lett.* **79**, 4375 (2001).
- <sup>15</sup>H. D. Sun, A. H. Clark, S. Calvez, M. D. Dawson, K. S. Kim, T. Kim, and Y. J. Park, *Appl. Phys. Lett.* **87**, 021903 (2005).
- <sup>16</sup>B. Y. Homan, R. B. Seth, B. Hopil, A. W. Mark, and J. S. Harris, Jr., *J. Appl. Phys.* **99**, 093504 (2006).
- <sup>17</sup>Y. P. Varshni, *Physica (Amsterdam)* **34**, 149 (1967).
- <sup>18</sup>Z. M. Fang, K. Y. Ma, D. H. Jaw, R. M. Cohen, and G. B. Stringfellow, *J. Appl. Phys.* **67**, 7034 (1990).
- <sup>19</sup>M. A. Pinault and E. Tournie, *Appl. Phys. Lett.* **78**, 1562 (2001).
- <sup>20</sup>A. Polimeni, M. Capizzi, M. Geddo, M. Fischer, M. Reinhardt, and A. Forchel, *Appl. Phys. Lett.* **77**, 2870 (2000).
- <sup>21</sup>M. Merrick, S. A. Cripps, B. N. Murdin, T. J. C. Hosea, T. D. Veal, C. F. McConville, and M. Hopkinson, *Phys. Rev. B* **76**, 075209 (2007).
- <sup>22</sup>H. D. Sun, S. Calvez, M. D. Dawson, J. A. Gupta, G. I. Sproule, X. Wu, and Z. R. Wasilewski, *Appl. Phys. Lett.* **87**, 181908 (2005).
- <sup>23</sup>Y. Z. Gao, X. Y. Goings, and T. Yamaguchi, *Jpn. J. Appl. Phys., Part 1* **45**, 5732 (2006).
- <sup>24</sup>X. Yang, J. B. Heroux, M. J. Jurkovic, and W. I. Wang, *Appl. Phys. Lett.* **76**, 795 (2000).
- <sup>25</sup>A. Guzmán, E. Luna, F. Ishikawa, and A. Trampert, *J. Cryst. Growth* **311**, 1728 (2009).